Band structure of superlattice with graded interfaces

H. X. Jiang and J. Y. Lin

Citation: Journal of Applied Physics **61**, 624 (1987); doi: 10.1063/1.338214
View online: http://dx.doi.org/10.1063/1.338214
View Table of Contents: http://scitation.aip.org/content/aip/journal/jap/61/2?ver=pdfcov
Published by the AIP Publishing

Band structure of superlattice with graded interfaces

H. X. Jiang[a] and J. Y. Lin
Department of Physics, Syracuse University, Syracuse, New York 13244-1130

(Received 25 July 1986; accepted for publication 6 October 1986)

The electron-energy levels in the GaAs-$Ga_{1-x}Al_xAs$ superlattice with finite thicknesses of interfaces between the layers, instead of sharp discontinuities across the interfaces, have been investigated. This model is more realistic for superlattices. A linearly increased (decreased) potential across the interfaces was assumed and a dispersion relation was derived to the second order of the thickness of the interface. The miniband structure, the shifting of the ground-state energy of the electron, and the effective-energy gap as functions of this thickness are presented.

I. INTRODUCTION

With recent advances in epitaxial-crystal-growth techniques, it has become possible to grow the semiconductor superlattice system composed of alternate layers of two different materials with controlled thicknesses, many of which are currently under study due to their interesting properties, such as negative resistance.[1,2] Another interesting property is the formation of the minibands. There are numerous published articles in this field.[3–9] The most extensively studied superlattice is the one consisting of alternate layers of GaAs and $Ga_{1-x}Al_xAs$. The GaAs layers form quantum wells and the $Ga_{1-x}Al_xAs$ layers form potential barriers. For Al concentration less than about 40% ($x<0.4$), $Ga_{1-x}Al_xAs$ has a direct band gap at the Γ point.[8]

In addition to the superlattices with the usual structure, the superlattices with more complex structures such as polytype (ABC) superlattices,[10] sawtooth superlattices,[11,12] effective-mass superlattices,[13] and binary superlattices consisting of multiple alternating layers per period[14] have been proposed. These complex structures provided additional degrees of freedom, so that more parameters would be available for obtaining the desired electronic and optical properties. Most papers in this field assumed that the interfaces between the layers are sharply defined with zero thicknesses so as to be devoid of any interface effect; the superlattice potential distribution may be considered simply as a one-dimensional array of rectangular wells. Advanced experimental techniques such as chemical vapor deposition, liquid-phase epitaxy, and molecular-beam epitaxy may produce superlattices with physical interfaces between two materials crystallographically abrupt, but the bonding environment of the atoms adjoining this interface will change on at least an atomic scale. As the potential form changes from a well (barrier) to a barrier (well), an intermediate potential region exists for the electrons and the holes. Naturally, the question arises as to what is the miniband structure if we consider the existence of finite thicknesses of the interfaces so that potential forms for the electrons and holes are continuous. The heterojunction effect was modeled using a graded interface by Stern and Sarma.[15] They used an approximation treatment (tight binding) to calculate the electron-energy levels in GaAs-$Ga_{1-x}Al_xAs$ heterojunctions. In this paper, calculated results of electron-energy levels in the GaAs-$Ga_{1-x}Al_xAs$ superlattice are presented for graded interfaces, which have not been previously treated. We obtained the dependencies of the miniband structure and the effective-energy gap of the superlattice on the thickness of the interface between the layers, and found that the corrections due to this interface are quite significant (several meV). The effect of the interface on the electron ground-state energy is also presented. For simplicity, we consider only the case of small Al concentration, so that the assumption of a single effective mass of the electron (hole) for the two materials is valid.

II. CALCULATIONS

Figure 1 is the band profile of the superlattice with graded interfaces between the layers showing the periodic potential arising from the band-gap difference between the well and barrier materials. We have a periodic potential with four different potential regions in each period, which can be written as

$$V=\begin{cases} p(x-nL), & 0\leqslant x-nL<\Delta, \\ V_0, & \Delta\leqslant x-nL<a, \\ p[a-(x-nL)]+V_0, & a\leqslant x-nL<a+\Delta, \\ 0, & a+\Delta\leqslant x-nL<L, \end{cases} \quad n=0,1,2..., \tag{1}$$

where a and b are, respectively, the widths of the barrier and well, $L(=a+b)$ is the period length, Δ is the thickness of the interface, which depends on the materials and the condi-

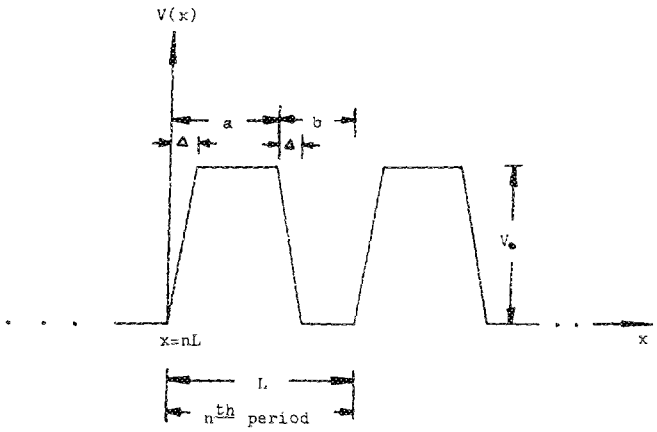

FIG. 1. Band profile of the superlattice with finite widths of the interfaces between the layers showing the periodic potential arising from the band-gap difference between the well and barrier materials.

[a] Present address: Center for Fundamental Material Research; Michigan State University, East Lansing, MI 48824. Address correspondence to this author.

 0021-8979/87/020624-05$02.40

tion of the interfaces, and p is the slope of the linear potential with $p\Delta = V_0$.

From the Schrödinger equation

$$(-\hbar^2/2m)\frac{d^2\psi}{dx^2} + V\psi = E\psi\,, \tag{2}$$

we can immediately get the wave function in the constant-potential regions of the nth period.

$$\psi_2(x) = C_n \exp[k(x-nL)] + D_n \exp[-k(x-nL)]\,, \quad (\Delta \leqslant x - nL < a), \tag{3a}$$

$$\psi_4(x) = G_n \exp[ik'(x-nL)] + H_n \exp[-ik'(x-nL)]\,, \quad (a+\Delta \leqslant x - nL < L).$$

In the interface regions of the nth period, with a proper coordinate transformation,[16] we get as solutions the Airy functions $\mathrm{Ai}(x)$ and $\mathrm{Bi}(x)$,[17]

$$\psi_1(x) = A_n\,\mathrm{Ai}[Z(x-nL)] + B_n\,\mathrm{Bi}[Z(x-nL)]\,, \quad (0 \leqslant x - nL < \Delta)\,, \tag{3b}$$

$$\psi_3(x) = E_n\,\mathrm{Ai}[Z'(x-nL)] + F_n\,\mathrm{Bi}[Z'(x-nL)]\,, \quad (a \leqslant x - nL < a+\Delta)\,.$$

In Eq. (3), $A_n, B_n, \ldots, H_n$, $n = 0, 1, 2, \ldots$, are the constant coefficients of the wave function in the nth period, and

$$Z(x) = \alpha_1^{1/3}x - \tilde{\epsilon}\alpha_1^{-2/3}\,,$$

$$Z'(x) = \alpha_2^{1/3}x - \tilde{\epsilon}'\alpha_2^{-2/3} = -Z(x) - (2m/\hbar^2)(V_0 + pa)\,,$$

$$\alpha_1 = 2mp/\hbar^2\,,$$

$$\alpha_2 = -\alpha_1\,,$$

$$\tilde{\epsilon} = k'^2 = 2mE/\hbar^2\,,$$

$$\tilde{\epsilon}' = \tilde{\epsilon} - (2m/\hbar^2)(V_0 + pa) = (2m/\hbar^2)(E - V_0 - pa)\,,$$

$$k = [2m(V_0 - E)]^{1/2}/\hbar\,. \tag{4}$$

Here, we assume that the effective mass of the electron m is the same for the two materials. Using the matrix method[18] and the continuity conditions of the wave function and its derivative across the interfaces, we get the following expression:

$$\begin{pmatrix} G_n \\ H_n \end{pmatrix} = M \begin{pmatrix} G_{n-1} \\ H_{n-1} \end{pmatrix} = M^n \begin{pmatrix} G_0 \\ H_0 \end{pmatrix}, \tag{5}$$

$$M = Q_4^{-1}P_4P_3^{-1}Q_3Q_2^{-1}P_2P_1^{-1}Q_1\,, \tag{6}$$

$$P_j = \begin{pmatrix} \mathrm{Ai}(R_j) & \mathrm{Bi}(R_j) \\ \mathrm{Ai}'(R_j) & \mathrm{Bi}'(R_j) \end{pmatrix}, \quad (j = 1, 2, 3, 4)\,, \tag{7a}$$

$$Q_j = \begin{pmatrix} \exp(k_jx_j) & \exp(-K_jx_j) \\ K_j\exp(K_jx_j) & -K_j\exp(-K_jx_j) \end{pmatrix}, \quad (j = 2, 3, 4)\,, \tag{7b}$$

where $R_j = Z_j = Z(x_j)$ for $j = 1$, and 2; $R_j = Z_j' = Z'(x_j)$ for $j = 3$, and 4; $K_j = k$ for $j = 2$, and 3, and $K_j = ik'$ for $j = 4$. In Eqs. (7a) and (7b), $x_1 = 0$, $x_2 = \Delta$, $x_3 = a$, $x_4 = a + \Delta$, and $\mathrm{Ai}'(R)[\mathrm{Bi}'(R)]$ is the derivative of $\mathrm{Ai}(R_j)[\mathrm{Bi}(R_j)]$ with respect to x at $x = x_j$. For Q_1 we have,

$$Q_1 = \begin{pmatrix} \exp(ik'L) & \exp(-ik'L) \\ ik'\exp(ik'L) & -ik'\exp(-ik'L) \end{pmatrix}. \tag{7c}$$

Also, from the properties of Airy functions, we have the condition[19]

$$\mathrm{Ai}(x)\mathrm{Bi}'(x) - \mathrm{Ai}'(x)\mathrm{Bi}(x) = \pi^{-1}\,. \tag{8}$$

From Eqs. (6) and (7), where we find that the determinant of matrix M is unity $|M| = 1$ and from that requirement, the wave function of the electron (hole) must be finite, we can define a real parameter q, which is related to the energy by the equation

$$\cos(qL) = \mathrm{Tr}\,M/2\,. \tag{9}$$

We can get an exact dispersion equation from Eqs. (6)–(9). However, the expression is very complicated and the physical meaning is not very clear. In the following calculations, we note that the interface thickness Δ is very small, so that $k\Delta$ and $k'\Delta$ are much less than 1. We will derive a dispersion relation to the second order of Δ.

From Eqs. (6)–(8), for small Δ, assuming $k\Delta \ll 1$ and $k'\Delta \ll 1$, we have, with the relation $Z_4' = Z_3' + \alpha_2^{1/3}\Delta$ and the utilization of the Taylor expansion up to the second order of $k\Delta$ and $k'\Delta$.

$$\mathrm{Qi}(Z_4') = \mathrm{Qi}(Z_3') + \alpha_2^{1/3}\Delta\,\mathrm{Qi}^*(Z_3') + (1/2)\alpha_2^{2/3}\Delta^2 Z_3' \times \mathrm{Qi}(Z_3') + (1/3)\alpha\Delta^3\,\mathrm{Qi}(Z_3')\,, \tag{10}$$

$$\mathrm{Qi}'(Z_4') = \alpha_2^{1/3}\{\mathrm{Qi}^*(Z_3') + \alpha_2^{1/3}\Delta Z_3'\,\mathrm{Qi}(Z_3') + (1/2)\alpha_2^{2/3}\Delta^2[\mathrm{Qi}(Z_3') + Z_3'\,\mathrm{Qi}^*(Z_3')] + (2/3)\alpha_2\Delta^3\,\mathrm{Qi}^*(Z_3')\}\,,$$

where Qi = Ai and Bi, and Qi* is the derivative of Qi with respect to Z' at $Z' = Z_i'$ $(i = 3, 4)$. In obtaining Eq. (10), the relation[17] $\mathrm{Qi}''(x) = x\,\mathrm{Qi}(x)$ was used. From Eqs. (7a), (8), and (10), we have

$$P_4P_3^{-1} = \begin{pmatrix} 1 + (k^2 - 2k'^2)\Delta^2/6 & \Delta \\ (k^2 - k'^2)\Delta/2 & 1 - (k^2 + 4k'^2)\Delta^2/6 \end{pmatrix}. \tag{11a}$$

By using the same method of calculation for matrices P_2 and P_1^{-1} and expanding $\mathrm{Ai}(Z_2)$, $\mathrm{Bi}(Z_2)$, $\mathrm{Ai}'(Z_2)$, and $\mathrm{Bi}'(Z_2)$ at $Z = Z_1$, keeping the terms up to the second order of $k\Delta$ and $k'\Delta$, we obtain

$$P_2P_1^{-1} = \begin{pmatrix} 1 + (2k^2 - k'^2)\Delta^2/6 & \Delta \\ (k^2 - k'^2)\Delta/2 & 1 + (4k^2 + k'^2)\Delta^2/6 \end{pmatrix}. \tag{11b}$$

In obtaining Eq. (11), we notice that $\alpha_2^{2/3}Z_3' = k^2$, $-\alpha_2\Delta = \alpha_1\Delta = (k^2 + k'^2)$, and $\alpha_1^{2/3}Z_1 = -k'^2$. From Eqs. (6), (7), and (11), we get the trace of M:

$$\mathrm{Tr}\,M = 2\cosh\beta\cos\gamma + \epsilon\sinh\beta\sin\gamma + \Delta\,[(k^2k'^{-1} - 3k')\cosh\beta\sin\gamma + (3k^2 - k'^2k^{-1})\sinh\beta\cos\gamma] + \Delta^2[2(k^2 - k'^2)\cosh\beta\cos\gamma + (1/12)(5k^3k'^{-1} + 5k'^3k^{-1} - 34kk')\sinh\beta\sin\gamma]\,, \tag{12}$$

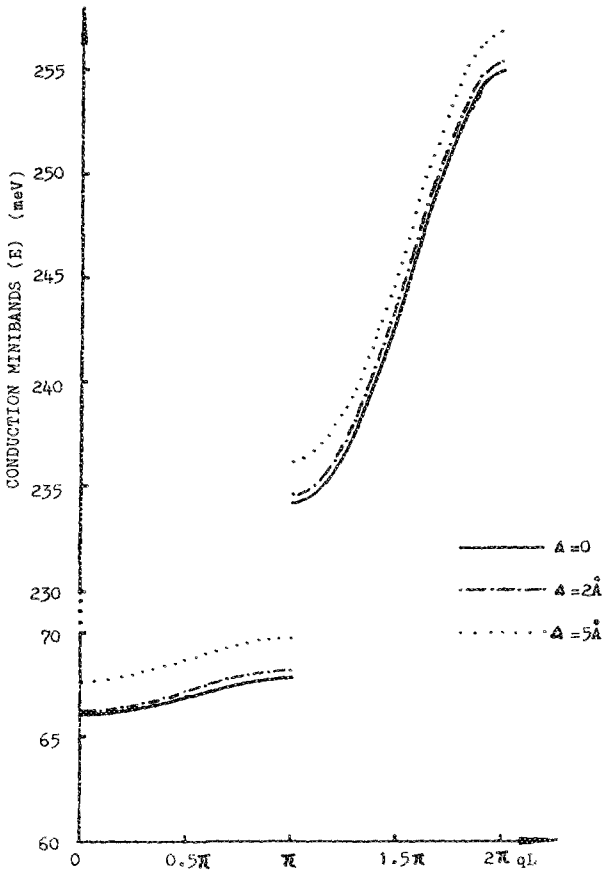

FIG. 2. Miniband structure of the GaAs-$Ga_{1-x}Al_xAs$ superlattice showing the first two allowed conduction minibands for three different values of the interface thicknesses with $L = 120$ Å, $a = b = L/2$, and $x = 0.3$.

where $\epsilon = kk'^{-1} - k'k^{-1}$, $\beta = k(a-\Delta)$, and $\gamma = k'(b-\Delta)$. Substituting Eq. (12) into Eq. (9), and keeping terms up to the second order of $k\Delta$ and $k'\Delta$, results in

$$\cos(qL) = [1 + (k'^2 - k^2)\Delta^2]\cosh(ka)\cos(k'b) + (\epsilon/2) \times [1 + (k'^2 - k^2)\Delta^2/12]\sinh(ka)\sin(k'b) . \quad (13)$$

Equation (13) is the dispersion relation of the electron (hole) obtained with the consideration of graded interfaces and is valid only for small Δ. We can see that the correction to the energy levels due to the first order of Δ is zero. From symmetry, the corrections due to the higher odd orders are also zero. By using the same techniques as were used in obtaining Eq. (13), the dispersion relation for higher orders of $k\Delta$ and $k'\Delta$ can easily be obtained. It is obvious that, when Δ goes to zero, Eq. (13) will reduce to the dispersion relation for the Kronig–Penney model.[16] We will use Eq. (13) to calculate the miniband structure of the GaAs-$Ga_{1-x}Al_xAs$ superlattice.

III. DISCUSSION

In our calculation, for a GaAs-$Ga_{1-x}Al_xAs$ superlattice, the empirical expression, $E_g = 1.155x + 0.37x^2$ eV, for the direct band-gap difference between GaAs and $Ga_{1-x}Al_xAs$[7–9] was used. The conduction and the valance-band discontinuities at the interface have been suggested to be about 85% and 15%, respectively, of the direct band-gap difference between the two semiconductor materials.[4,5,7,9] Using the Al concentration, $x = 0.3$, we get[20–23] $V_e = 0.3228$ eV and $V_h = 0.057$ eV. As an approximation, we have used $m_e = 0.08m_0$ for the average value of the electron effective mass, $m_{hh} = 0.48m_0$ for the heavy holes, and $m_{lh} = 0.09m_0$ for the light holes, where m_0 is the electron mass in free space. The next higher neglected order in Eq. (13) is $(k\Delta)^4$. Therefore, for $\Delta \leqslant 5$ Å, Eq. (13) is a very good approximation.

Figure 2 is the miniband structure of the GaAs-$Ga_{1-x}Al_xAs$ superlattice ($L = 120$ Å, $a = b = L/2$, and $x = 0.3$) showing the first two allowed conduction minibands for three different values of the interface thickness.

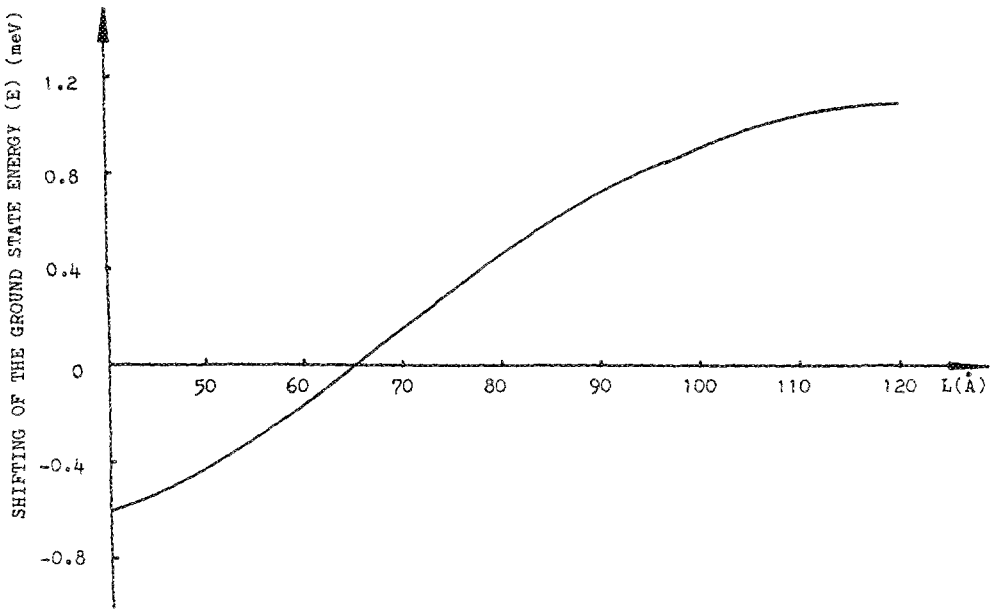

FIG. 3. Shift in the ground-state energy ($n = 1$, $q = 0$) between $\Delta = 4$ Å and $\Delta = 0$ as a function of the period length L with $a = b = L/2$ and $x = 0.3$.

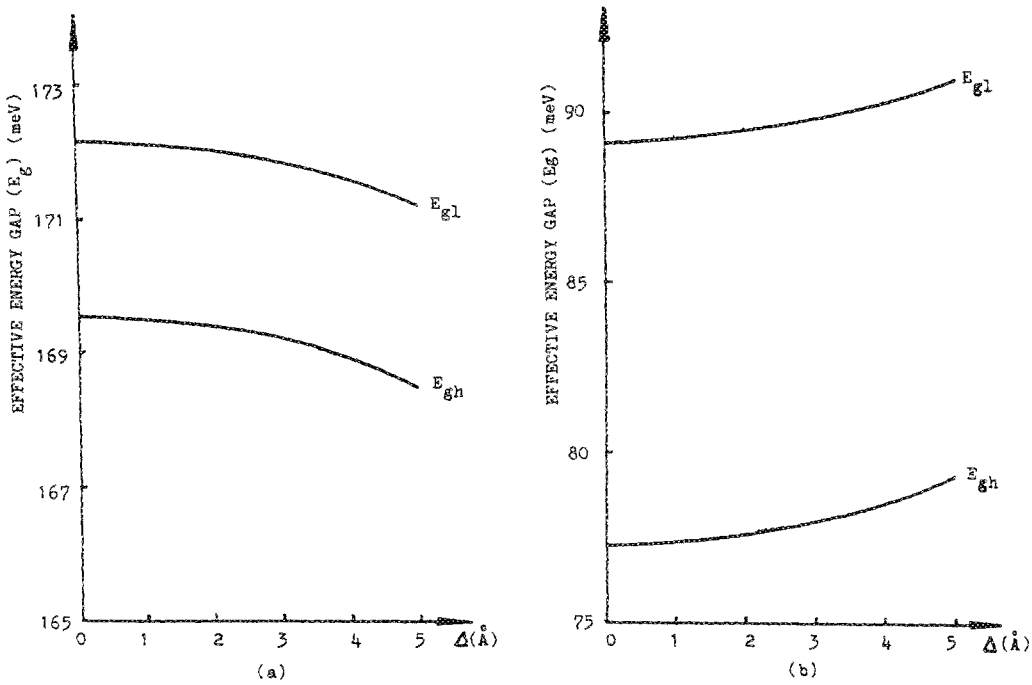

FIG. 4. Effective-energy gap vs Δ for both heavy (E_{gh}) and light (E_{gl}) holes with $a = b = L/2$ and (a) $L = 40$ Å, (b) $L = 120$ Å.

From Fig. 2, we see that the energy of the electron, for a fixed value of q, increases as Δ increases. For each value of q within a miniband, the energy increase due to the increase of the interface thickness Δ, is almost constant. In addition, the energy increase is larger in the second miniband than in the first miniband.

In Fig. 2, we plotted only the miniband structure for $L = 120$ Å. For more general cases, we can express the energy of an electron with wave number q in the nth miniband under the effect of the interfaces of thickness Δ as,

$$E_n(q,\Delta) = E_n(q,\Delta = 0) + F(n,q,\Delta,L) , \qquad (14)$$

where $E_n(q,\Delta = 0)$ is the electron energy with zero interface thickness, and $F(n,q,\Delta,L)$ is the shift of the electron energy due to the effect of the interface, which depends on n, the interface thickness Δ, and the period L, and only slightly on q. For $L = 120$ Å, F is positive. It is interesting to note that for small L ($L < 60$ Å), F is negative. It can be seen that the correction in the energy of the electron due to the interface strongly depends on the superlattice period L.

Figure 3 is a plot of the shift of the ground-state energy ($n = 1$, $q = 0$) between $\Delta = 4$ Å and $\Delta = 0$ as a function of the period length L (for $a = b = L/2$ and $x = 0.3$). In fact, this is also a plot of the function F vs L, with $n = 1$, $q = 0$, and $\Delta = 4$ Å. From Fig. 3, we can see that if period L varies from 40 to 65 Å, the ground-state energy of the electron will decrease due to the interface effect. If period L varies from 65 to 120 Å, the ground-state energy of the electron will increase. The maximum shift between $\Delta = 4$ Å and $\Delta = 0$, is about 1.1 meV at $L = 120$ Å. The shift increases almost linearly in the region of $L = 60$ to $L = 90$ Å.

The results in Fig. 3 can be understood if we note that the ground-state energy of the electron with a zero interface thickness depends on the period length L. For small L, the ground state lies close to the top of the potential well. Because of the interface effect, the effective-potential well for the electron, as shown in Fig. 1, becomes larger. This will cause the ground-state energy to decrease. For the same reason, the ground state of the electron lies close to the bottom of the well for larger L, and the effective-potential well becomes narrower due to the interface effect. This will cause the ground-state energy of the electron to increase. For superlattices with either small or large L, the interfaces cause significant changes in energy.

Figure 4 shows the plots of the effective-energy gaps as functions of Δ for both heavy (E_{gh}) and light (E_{gl}) holes for (a) $a = b = L/2$ with $L = 40$ Å and (b) $L = 120$ Å. Here, the effective-energy gap has been defined as the energy difference between the lowest conduction miniband and the uppermost valence miniband. As we have mentioned before, for $x = 0.3$, GaAs-$Ga_{1-x}Al_xAs$ superlattices have a direct band gap at the Γ point. If the Coulomb and phonon interactions are neglected, the effective-energy gap represents the minimum energy required for producing excitons.

From Fig. 4, we see that, for $L = 40$ Å, the effective-energy gap for both heavy (E_{gh}) and light holes (E_{gl}) will decrease if Δ increases. This is because the ground-state energy of the electron will decrease if Δ increases for $L = 40$ Å. For $\Delta = 0$ to 2 Å, the change of the effective-energy gap is small and for $\Delta = 3$ to 5 Å, it decreases more quickly. The plot of E_{gh} and E_{gl} are parallel to one another; this is because of the very small difference in the shift of the ground-state energies between the heavy and light holes. The energy gap between the heavy and light holes for the first valence miniband is about 2.6 meV for $\Delta = 0$ and 2.7 meV for $\Delta = 5$ Å. In contrast to Fig. 4(a), for $L = 120$ Å, the effective-energy gap for both the heavy and light holes will increase if Δ increases. It increases about 2.0 meV for E_{gh} and 1.2 meV for E_{gl} when Δ changes from 0 to 5 Å. The energy gap between the heavy and light holes for the first valence miniband is about 12.0 meV for $\Delta = 0$ and 11.6 meV for $\Delta = 5$ Å.

In conclusion, with the assumption of linear potentials

across the interfaces, we have investigated the interface effect on the miniband structure of the superlattice, and a simple dispersion relation to the second order of the interface thickness between the layers has been derived. The interesting result is that the effective-energy gap will either increase or decrease depending on the period length L of the superlattice. As indicated from the above calculations and discussions, we see that the interface effect on the miniband structure of the superlattice is important and cannot be neglected in many cases. The linear-potential form for the electron and hole across the interfaces is a good approximation. It also allows us to derive the dispersion relation from first principles. At this stage, the exact potential form for the electron and hole in the interface is unknown. More information from experiments is needed to determine the real potential form across the interfaces. The results obtained in this paper will be useful in technological applications and in basic research.

ACKNOWLEDGMENTS

We would like to thank Dr. Charles Wang and Dave Baum for their many helpful suggestions and critical reading of the manuscript.

[1]L. Esaki and R. Tsu, IBM J. Res. Dev. **14**, 61 (1970).
[2]R. Tsu and G. Dohler, Phys. Rev. B **12**, 680 (1975).
[3]L. L. Chang, L. Esaki, and R. Tsu, Appl. Phys. Lett. **24**, 593 (1974).
[4]D. Mukherji and B. R. Nag, Phys. Rev. B **12**, 4338 (1975).
[5]R. Dingle, W. Wiegmenn, and C. H. Henry, Phys. Rev. Lett. **33**, 827 (1974).
[6]G. H. Dohler, Phys. Scr. **24**, 430 (1981).
[7]R. L. Greene and K. K. Bajaj, Phys. Rev. B **31**, 913 (1984).
[8]H. J. Lee, L. Y. Juravel, J. C. Wolley, and A. J. Springthorpe, Phys. Rev. B **21**, 659 (1980).
[9]W. T. Masselink, Y.-C. Chang, and H. Morkoc, Phys. Rev. B **28**, 7373 (1983).
[10]L. Esaki, L. L. Chang, and E. E. Mendez, Jpn. J. Appl. Phys. **20**, L529 (1981).
[11]M. Jaros, K. B. Wong, and M. A. Gell, Phys. Rev. B **31**, 1205 (1985).
[12]J. A. Brum, P. Voisin, and G. Bastard, Phys. Rev. B **33**, 1063 (1986).
[13]A. Sasaki, Phys. Rev. B **30**, 7016 (1984).
[14]H. X. Jiang and J. Y. Lin, Phys. Rev. B **33**, 5851 (1986).
[15]F. Stern and S. D. Sarma, Phys. Rev. B **30**, 840 (1984).
[16]E. J. Austin and M. Jaros, Phys. Rev. B **31**, 5569 (1985).
[17]A. Rabinovitch and J. Zak, Phys. Rev. B **4**, 2358 (1971).
[18]E. Merzbacher, *Quantum Mechanics*, 2nd ed. (Wiley, New York, 1970), pp. 73–105.
[19]*Handbook of Mathematic Functions With Formula, Graphs, and Mathematical Table*, edited by M. Abramowitz and I. A. Stegun (N.B.S. Applied Mathematics Series, Washington, DC, 1964), pp. 446–447.
[20]C. Mailhiot, Y. C. Chang, and T. C. McGill, Phys. Rev. B **26**, 4449 (1982).
[21]C. Priester, G. Allan, and M. Lannoo, Phys. Rev. B **30**, 7302 (1984).
[22]*Heterostructure Lasers*, edited by H. C. Casey and M. B. Panish (Academic, New York, 1978), Part A, Chap. 4.
[23]T.-F. Siang, Solid State Commun. **50**, 589 (1984).